



Adsorption of reactive Orange 16 by Amberlyst A21: Isotherm and kinetic investigations

Murat Basar , Hülya Silah* 

Bilecik Şeyh Edebali University, Faculty of Art & Science, Department of Chemistry, 11210, Bilecik, Turkey

Abstract

Recently, Amberlyst A21 has attracted much attention because of its highly selective feature as well as its specific chemical and physical structure. In the present work, Amberlyst A21 polystyrene resin was used as a new sorbent for Reactive Orange 16 dye. The experimental conditions i.e. such solution pH, initial Reactive Orange 16 concentration, contact time, and Amberlyst A21 dosage were optimized using by batch adsorption technique. The morphology of surface and functional groups of Amberlyst A21 was investigated by using Scanning Electron Microscopy (SEM) and Fourier Transform Infrared Spectroscopy (FT-IR). The adsorption isotherm data indicate that the Langmuir isotherm model is the best fit model. The calculated maximum Reactive Orange 16 adsorption capacity of Amberlyst A21 was 175.13 mg g⁻¹. The pseudo-first and second-order kinetic models are used to clarify the mechanism of adsorptive removal by Amberlyst A21 in optimal experimental conditions were discussed. The reactive Orange 16 adsorption kinetics and equilibrium data were successfully defined by pseudo-first-order and Langmuir models, respectively. This manuscript currently shows an uncomplicated way of wastewater treatment and a new adsorbent for dye removal which might develop an environmental process based on the use of Amberlyst A21 resin.

Keywords: Adsorbent, isotherms, kinetics, Reactive Orange 16, resin

1. Introduction

Due to the growth of industrialization, a large number of wastewaters containing dyes that are used in various industrial areas is discharged into the environment. The organic pollutants such as dyes, which have led to various serious health and environmental problems, are difficult to be treated owing to they are easily outspreading through air or water into the ground, long-time degradation, and high treatment cost [1,2]. So that various chemical, physical and biological methods, including ozonation [3], advanced oxidation [4], adsorption [5,6], membrane filtration [7], flocculation/coagulation [8], biosorption [9], ion-exchange [10], and photocatalytic degradation [11] are often used to treat of wastewater including dyes and other contaminants. Among these methods, adsorption was so attractive because of convenience and low-cost in application [12]. Nowadays, the adsorption technique is most commonly applied for wastewater purification due to its yield in the

removal of various pollutants too stable for biological methods [13].

Azo dyes, which are characterized by the presence of -N=N- chromophore groups in the complex chemical structure, are widely available textile, plastic, cosmetic, paper, leather, and food industry [14]. Reactive Orange 16 (Fig.1), a synthetic azo compound, is mostly used in various industrial areas. The discharge of wastewater containing Reactive Orange 16 causes serious biotic risk in the environmental media [15].

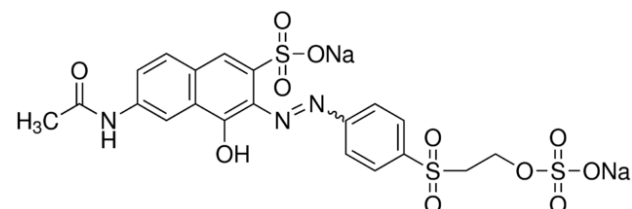


Figure 1. Chemical structure of Reactive Orange 16.

In this paper, Amberlyst A21 resin was selected as the sorbent due to its highly selective properties as

well as its specific chemical and physical structure so; removal of some pollutants as palladium (II) [17], acetic acid [18,19], butyric and oxalic acids [19] sulfate [16], chromium (VI) [20] have been investigated by using Amberlyst A21.

The present manuscript aims to explore the adsorption efficiency of Amberlyst A21 polystyrene resin for the removal of Reactive Orange 16 dye from wastewaters. FT-IR and SEM techniques are used to characterize the structure of Amberlyst A21 resin. The optimal adsorption conditions were defined by the experiments of pH, adsorption time, amount of Amberlyst A21, and initial Reactive Orange 16 concentrations. Langmuir, Freundlich, and Temkin isotherm were utilized to comply with equilibrium adsorption data and evaluate the adsorption behaviour of Reactive Orange 16. In addition, the experimental data were tested with kinetic models to determine the rate-controlling mechanism for the dye adsorption process. In the literature, there are very few studies about the removal of dyes with Amberlyst A21. The recommended removal process for Reactive Orange 16 has superiorities such as a simple way of operation and high efficiency to remove the dye in a short time.

2. Experimental

2.1. Materials

Amberlyst A21 and Reactive Orange 16 dye used for this study were provided from Sigma-Aldrich. Hydrogen chloride (HCl), sodium hydroxide (NaOH), and other chemicals used were of analytical grade from Merck and were used without further purification. All solutions were prepared with deionized water.

2.2. Morphological analysis of adsorbent

Fourier transform infrared spectroscopy (FT-IR) and scanning electron microscopy (SEM) were used to characterize Amberlyst A21. The FT-IR spectroscopy analyses were recorded on Perkin Elmer, Spectrum 100 Model over the range of 400-4000 cm^{-1} with ATR technique in the range resolution of 4 cm^{-1} . Scanning electron microscopy (Zeiss Supra 40 V device) was used to observe the internal and surface morphologies of Amberlyst A21.

2.3. Batch adsorption characteristics of Reactive Orange 16

In adsorption studies, all Reactive Orange 16 solutions were prepared by diluting the stock dye solution (1000 mg L^{-1}) with the appropriate volume of

deionized water. The pH value of aqueous solutions was set with HCl (0.1 M) or NaOH (0.1 M). All adsorption experiments were carried out in 100 mL Erlenmeyer flask with constant agitation at 100 rpm and room temperature (25 °C) for batch experiments. The effects of solution pH (2.0-10.0), Amberlyst A21 dose (0.25-2.00 g L^{-1}), contact times (5-200 minutes), and initial Reactive Orange 16 concentrations (50-300 mg L^{-1}) were investigated for removal process of dye. The concentration of the Reactive Orange 16 dye in aqueous solutions was examined with a UV-Vis spectrophotometer (T80 model-PG Instruments) by measuring the molar absorbance at 494 nm [24]. The equations (1) and (2) can be used to calculate the adsorption capacity (q_e , mg g^{-1}) of adsorbent and removal percentage (R %), respectively;

$$q_e = \frac{(C_0 - C_e)}{m} x V \quad (1)$$

$$\text{Removal (\%)} = \frac{(C_0 - C_e)}{C_0} x 100 \quad (2)$$

where m and V are the weight of adsorbent in gram and volume of dye solution in a liter, respectively. C_0 (mg L^{-1}) is the initial dye concentration and C_e (mg L^{-1}) is the dye ion concentration in the adsorption equilibrium state.

2.4. Isotherm and kinetics investigations

The adsorption isotherms and kinetic are crucial investigations in the design of removal systems of pollutants from wastewaters. For the adsorption experiments, three isotherm models, which included Freundlich, Langmuir, and Temkin models were applied to fit the experimental adsorption data. Kinetic models of pseudo-first and pseudo-second-order model were investigated to understand the adsorption behaviour of Reactive Orange 16 onto Amberlyst A21 and to assess the rate of adsorption.

3. Results and discussions

3.1. Morphological analysis

To further analyze the functional groups of the Amberlyst A21 surface, FT-IR spectra were utilized to characterize and described in Fig. 2.

FT-IR spectra obtained from free Amberlyst A21 resin showed (Fig. 2a) specific peaks at 2935 cm^{-1} and 2857 cm^{-1} correspond to C-H bonds stretching of alkane. The peak at 1362 cm^{-1} present in the spectrum (a) related to the C-N stretch in the amine group.

There is also band corresponding to aromatic stretching of C=C located at 1600-1400 cm^{-1} . The vibrations of =C-H bending are in the range of 1000-675 cm^{-1} [21]. In comparison to the spectra of Amberlyst A21 before and after adsorption of Reactive Orange 16, a significant shift in the spectral peaks was observed in 3000-2850 and 1680-1600 cm^{-1} . Also, as seen from Fig. 2, the band was shown at 1456 cm^{-1} before adsorption but after adsorption, this band was shifted to 1493 cm^{-1} . These shifts were occurred owing to the binding of Reactive Orange 16 ions with functional groups of Amberlyst A21. Thus, the changing of wavenumber of peaks confirms the adsorption of Reactive Orange 16 on the surface of Amberlyst A21.

16 sorption by Amberlyst A21, various pH values from 2.0 to 10.0 were tested. As shown in Fig. 4, when the pH value was 2.0, the maximum removal efficiency (90.58%) was achieved. And with the rise of pH value, the removal percent of Reactive Orange 16 decreases gradually to pH 8.0. This behavior can be explained by the electrostatic interactions between anionic Reactive Orange 16 dye and positively charged Amberlyst A21 surface $[\text{R-NH}_3(\text{Amberlyst}) + \text{H}_2\text{O} \leftrightarrow \text{RNH}_4^+(\text{Amberlyst}) + \text{OH}^-(\text{aqueous})]$ [16]. As solution pH increased from 2.0 to 4.0, the removal efficiency significantly reduced from 90.58% to 65.22%.

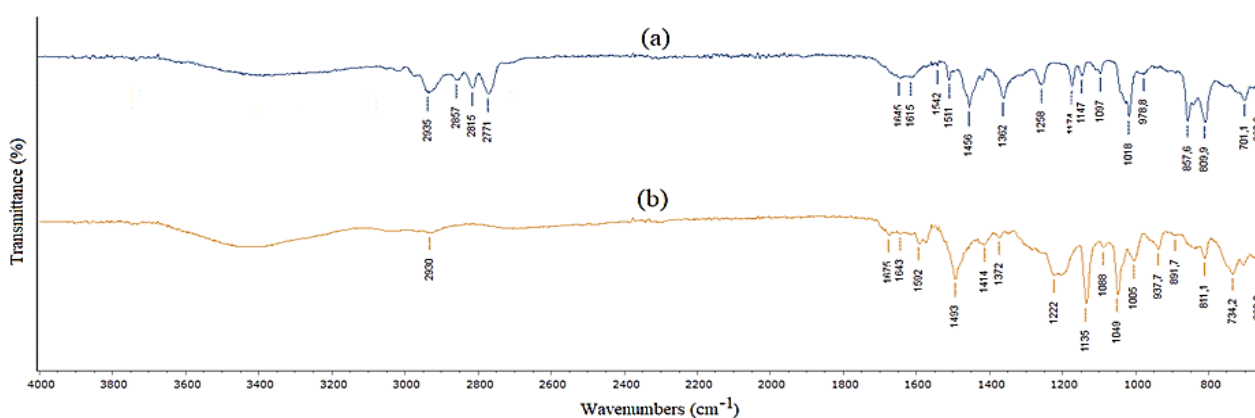


Figure 2. FT-IR spectra of (a) naked Amberlyst A21 and (b) Reactive Orange 16-Adsorbed Amberlyst A21.

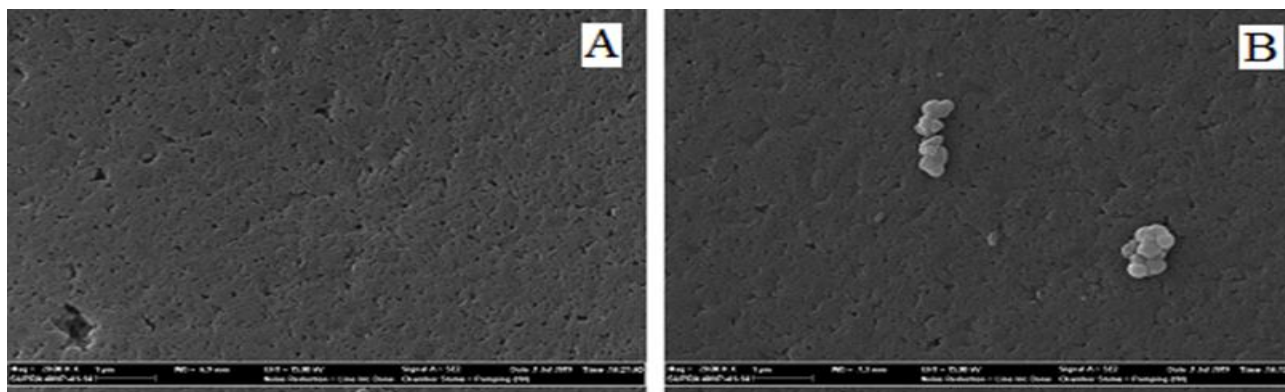


Figure 3. SEM images of (a) Reactive Orange 16 unloaded Amberlyst A21 and (b) Reactive Orange 16 loaded Amberlyst A21 resin.

Fig. 3 shows SEM images of Amberlyst A21 resin before (A) and after adsorption (B), indicating that the surface of Amberlyst A21 had a large surface area and rough porous structure.

3.2. Effect of solution pH and contact time

The solution pH plays an important role on the removal of dyes during the adsorption process because pH affects ionic forms of Reactive Orange 16 molecule and Amberlyst A21 surface charge. To reveal the optimum pH value for the Reactive Orange

The decrease in the adsorption of Reactive Orange 16 at pH greater than 2.0 can be related to the decrease of the positively charged sites of the Amberlyst A21 surface at a basic medium. Moreover, at higher pH values, the lower dye adsorption onto Amberlyst A21 can be linked to the large number of hydroxyl ions present, which compete with the negative dye groups for the adsorption binding sites of the resin. Further solution pH increased (4.0-10.0) removal percent of Reactive Orange 16 did not change remarkably. It is seen that this experimental result is consistent with the literature [16].

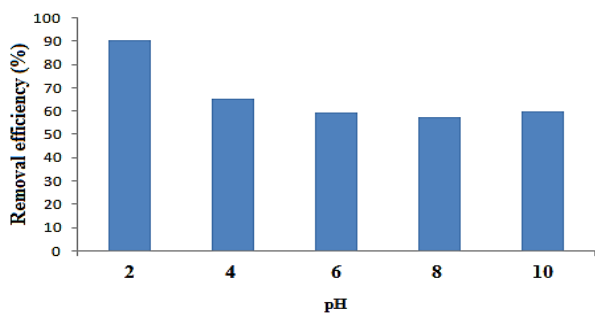


Figure 4. Effect of solution pH on the removal efficiency of Reactive Orange 16 using by Amberlyst A21 ($C_0=100 \text{ mg L}^{-1}$, adsorbent dosage= 1.0 g L^{-1}).

An important experimental factor that vigorously affects the adsorption of contaminants is the contact time. The effects of contact time on the removal of Reactive Orange 16 using by Amberlyst A21 was investigated in the range of 5-200 minutes at 100 mg L^{-1} initial Reactive Orange 16 solution at pH 2.0. The increasing dye removal percent with increasing contact time. After 180 minutes, curve of adsorption percentage tended to flat and no obvious change on the adsorption percentage of Reactive Orange 16 was observed. Therefore, the optimal contact time for Reactive Orange 16 adsorption on Amberlyst A21 was determined as 180 minutes for further removal studies.

3.3. Effect of Amberlyst A21 dose

The adsorbent dose is another important experimental condition for removing dyes from wastewaters and it determines the uptake capacity of adsorbents. The removal of Reactive Orange 16 was studied by varying the Amberlyst A21 dose from 0.25 to 2.00 g L^{-1} at other optimum experimental conditions. Adsorbent dosage increased from 0.75 to 2.00 g L^{-1} ; the percent removal of 100 mg L^{-1} Reactive Orange 16 increased from 73.42 to 100.00 for Amberlyst A21. This can be attributed to the increased surface area of adsorbent and availability of more binding sites as the adsorbent dosage increases [22]. In this study, the Amberlyst A21 dose was selected as 1.0 g L^{-1} with the percent removal of 90.58% .

3.4. Effect of the initial Reactive Orange 16 concentration

The effect of the initial Reactive Orange 16 concentration on the removal performance of Amberlyst A21 was studied in the concentration range from 50 to 300 mg L^{-1} using by 1.00 g L^{-1} Amberlyst A21 dosage at $25 \text{ }^\circ\text{C}$. The percent adsorption decreased with an increase in initial Reactive Orange 16 concentration. With the increase

of the initial concentration of Reactive Orange 16 from 50 to 300 mg L^{-1} , the adsorption capacity of Amberlyst A21 was greatly increased from 46.46 to 161.44 mg g^{-1} . However, when the concentration of dye increases further, the growth rate of adsorption decreases.

3.5. Adsorption isotherm study

The adsorbate-adsorbent interactions can be easily estimated by plotting the adsorption data into equilibrium isotherm models and the isotherm models help in understanding the designing of adsorption systems [23]. In the present work, three isotherm models, Langmuir, Freundlich, and Temkin were used to define the most appropriate isotherm model for the adsorption of Reactive Orange 16 onto Amberlyst A21. The Langmuir isotherm model is one of the most frequently used models in adsorption to describe the adsorption of adsorbate onto solid adsorbent surface. This isotherm model assumes that the adsorption takes place on an even monolayer surface with no layer interaction [24,25]. Also, the maximum adsorption capacity (q_m) of adsorbents can be studied by the Langmuir adsorption isotherms. The Langmuir isotherm equation can be given as follows [26]:

$$\frac{C_e}{q_e} = \frac{C_e}{q_m} + \frac{1}{q_m K_L} \quad (3)$$

Freundlich isotherm supposes that adsorption occurs on heterogeneous surfaces and according to this model different sites having different adsorption energies are involved during the adsorption process [27,28]. The equation of the Freundlich isotherm model is given as follows;

$$\log q_e = \log K_F + \frac{1}{n} \log C_e \quad (4)$$

The Temkin isotherm model assumes that the heat of the adsorption of all molecules in the layer decreases linearly with the surface of adsorbent coverage due to adsorbate-adsorbent interactions [29]. The Temkin isotherm model is given by the following equation;

$$q_e = A \ln K_T + A \ln C_e \quad (5)$$

In these equations; q_m is the maximum adsorption capacity (mg g^{-1}), A is the constant related to the heat of adsorption, K_T is the Temkin isotherm equilibrium

binding constant, K_L is the Langmuir constant ($L\text{ mg}^{-1}$), K_F is the Freundlich constant and n is a parameter related to adsorbate-adsorbent affinity.

Equilibrium isotherm of Reactive Orange 16 on Amberlyst A21 was obtained at pH 2.0 and 25 °C. The Langmuir, Freundlich, and Temkin adsorption parameters calculated for Reactive Orange 16 are presented in Table 1 and Fig. 5.

The coefficient value (R^2) for the Langmuir isotherm model was over 0.990, as shown in Table 1, higher than that for Freundlich and Temkin isotherm model, suggesting the adsorption isotherm of Reactive Orange 16 onto Amberlyst A21 fits the Langmuir isotherm model.

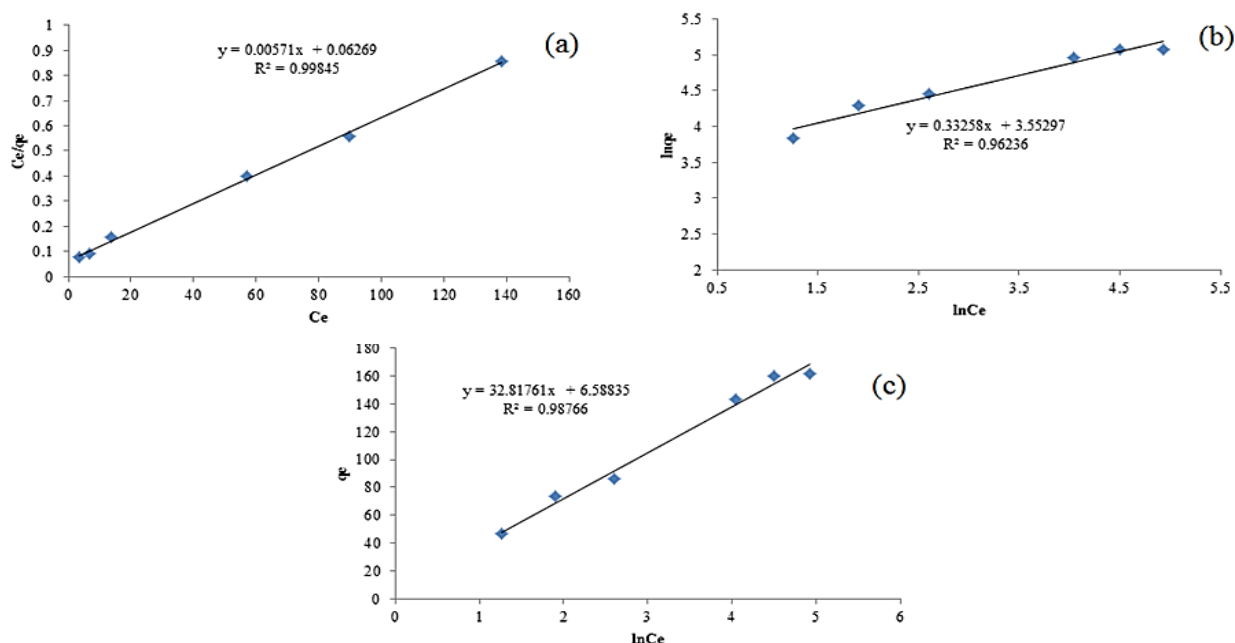


Figure 5. Isotherm models of (a) Langmuir, (b) Freundlich, and (c) Temkin for the adsorption of Reactive Orange 16 on Amberlyst A21

According to this result, during the adsorption process, the uptake of Reactive Orange 16 occurs on a homogenous surface by monolayer adsorption without any interaction between adsorbed dyes molecules [22].

Table 1. Isotherm parameters of Langmuir, Freundlich and Temkin models for Reactive Orange 16 adsorption on Amberlyst A21.

Langmuir	R^2	q_m	K_L	
	0.9985	175.13	0.09	
Freundlich	R^2	$1/n$	n	K_F
	0.9624	0.3326	3.01	34.92
Temkin	R^2	A	K_T	
	0.9877	32.82	1.22	

The maximum adsorption capacity q_m determined from the Langmuir isotherm defines the total capacity of the Amberlyst A21 for the Reactive Orange 16 as 175.13 mg g^{-1} .

The value of R_L is one of the most important parameters of the Langmuir isotherm and is called a separation factor. This dimensionless constant parameter of Reactive Orange 16 was obtained according to the Equation (6);

$$R_L = \frac{1}{1 + K_L C_0} \quad (6)$$

where C_0 is the initial Reactive Orange 16 concentration and K_L is a Langmuir isotherm constant. In this regard, the dimensionless constants were calculated as 0.035-0.099 for dye, suggesting that the adsorption process is favorable [5] and Amberlyst A21 can be used for dye removal.

3.6. Adsorption kinetic study

Adsorption kinetic investigations are very important with respect to defining the adsorption rate, which is one of the parameters used to determine adsorbent performance and to verify the adsorption mechanism considering a rate-limiting step.

The kinetics of Reactive Orange 16 adsorption was investigated by pseudo-first and second-order kinetics model according to following equations, respectively [30].

$$\log(q_e - q_t) = -\frac{k_1}{2.303}t + \log q_e \quad (7)$$

$$\frac{t}{q_t} = \frac{1}{k_2 q_e^2} + \frac{1}{q_e} t \quad (8)$$

where q_t (mg g^{-1}) and q_e (mg g^{-1}) are adsorption capacity at time (t) and equilibrium adsorption capacity, respectively. k_1 (min^{-1}); the rate constant of pseudo-first-order model was calculated from the slope of the plots of $\log(q_e - q_t)$ versus t . k_2 is the pseudo-second-order rate constant in ($\text{g mg}^{-1} \text{min}$) and this constant is calculated from the intercept of the plots of t/q_t versus t .

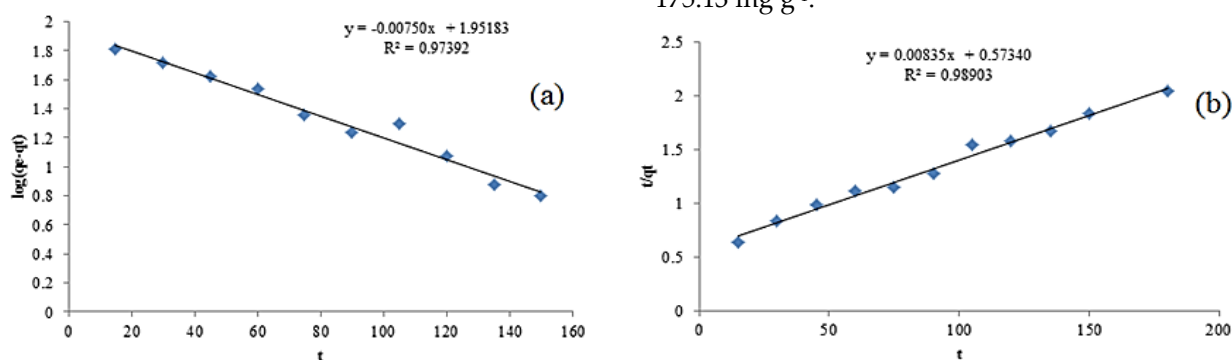


Figure 6. Adsorption kinetic graphs of Reactive Orange 16 onto Amberlyst A21 (a) pseudo first order and (b) pseudo second order kinetic model.

The fitted curves of the experimental adsorption data of two kinetic models were given in Fig. 6, and the calculated kinetic parameters were tabulated in Table 2. Kinetic parameters of Reactive Orange 16 on Amberlyst A21 were obtained at pH 2.0 and 25 °C.

Table 2. The adsorption kinetic constants of the Amberlyst A21 to Reactive Orange 16.

Amberlyst A21	Pseudo first order kinetic model				Pseudo second order kinetic model		
	$q_{e_{exp}}$ (mg g^{-1})	$q_{e_{cal}}$ (mg g^{-1})	k_1 (min^{-1})	R^2	$q_{e_{cal}}$ (mg g^{-1})	k_2 ($\text{g mg}^{-1} \text{dak}^{-1}$)	R^2
	86.50	89.50	1.73×10^{-2}	0.9739	119.76	1.21×10^{-4}	0.9890

The value of correlation coefficient, R^2 , for the pseudo-first-order kinetic model is relatively high and the theoretical adsorption capacity calculated ($q_{e_{cal}}$) by the kinetic equation (89.50 mg g^{-1}) is also very close to the determined value (86.50) by adsorption experiment ($q_{e_{exp}}$) for 100 mg L^{-1} Reactive Orange 16. The results indicate that the pseudo-first-order model is more suitable for Amberlyst A21 resin to adsorption of Reactive Orange 16 dye from aqueous solutions because of consistency between

the obtained and theoretical q_e values and higher correlation coefficients.

4. Conclusion

The adsorption properties of Amberlyst A21 resin was studied by removal of Reactive Orange 16 azo dye from aqueous solutions, and the solution pH dependence of adsorption was also investigated in this manuscript.

The experimental results indicated the optimal pH for maximum adsorption was 2.0 at 25 °C. Under optimal adsorption conditions pH 2.0, adsorbent dosage 1.0 g L^{-1} and 180 minutes contact time the maximum adsorption capacity was determined as 175.13 mg g^{-1} .

The adsorption isotherm studies showed that the adsorption of Reactive Orange 16 corresponded well with the Langmuir isotherm model. Also, the R_L values represented that adsorption of dye onto Amberlyst A21 was favorable. The investigation of adsorption kinetic data indicated that the proposed adsorption process could be described as a pseudo-first-order kinetic model with k_1 and q_e of $1.73 \times 10^{-2} \text{ min}^{-1}$ and 89.50 mg g^{-1} , respectively. Also, the results of this study show a simple way of wastewater treatment and a new adsorbent for dye removal which might develop an environmental process based on the use of Amberlyst A21 resin.

References

- [1] J.W. Kang, Removing environmental organic pollutants with bioremediation and phytoremediation, *Biotechnol Lett*, 36, 2014, 1129-1139.
- [2] H. Xie, X. Xiong, A porous molybdenum disulfide and reduced graphene oxide nanocomposite ($\text{MoS}_2\text{-rGO}$) with high adsorption capacity for fast and preferential adsorption towards Congo red, *J Environ Chem Eng*, 5(1), 2017, 1150-1158.

- [3] S. Venkatesh, A.R. Quaff, N.D. Pandey, K. Venkatesh, Decolorization and mineralization of C.I. direct red 28 azo dye by ozonation, *Desalin Water Treat*, 57(9), 2016, 4135-4145.
- [4] G.G. Bessegato, J.C. Souza, J.C. Cardoso, M.V.B. Zanoni, Assessment of several advanced oxidation processes applied in the treatment of environmental concern constituents from a real hair dye wastewater, *J Environ Chem Eng*, 6(2), 2018, 2794-2802.
- [5] B. Satılmış, T. Uyar, Amine modified electrospun PIM-1 ultrafine fibers for an efficient removal of methyl orange from an aqueous system, *Appl Surf Sci*, 453, 2018, 220-229.
- [6] U.D. Gül, H. Silah, Comparison of color removal from reactive dye contaminated water by systems containing fungal biosorbent, active carbon and their mixture, *Water Sci Technol*, 70(7), 2014, 1168-1174.
- [7] N. Nikoee, E. Saljoughi, Preparation and characterization of novel PVDF nanofiltration membranes with hydrophilic property for filtration of dye aqueous solution, *Appl Surf Sci*, 413, 2017, 41-49.
- [8] M. Chenna, R. Chemlal, N. Drouiche, K. Messaoudi, H. Lounici, Effectiveness of a physicochemical coagulation/flocculation process for the pretreatment of polluted water containing Hydron Blue Dye, *Desalin Water Treat*, 57, 2016, 27003-27014.
- [9] J. Chukki, S. Shanthakumar, Optimization of malachite green dye removal by *Chrysanthemum Indicum* using response surface methodology, *Environ Prog Sustain*, 35(5), 2016, 1415-1419.
- [10] M. Wawrzekiewicz, Z. Hubicki, E. Polska-Adach, Strongly basic anion exchanger Lewatit MonoPlus SR-7 for acid, reactive, and direct dyes removal wastewaters, *Sep Sci Technol*, 53(7), 2018, 1065-1075.
- [11] K.M. Reza, A.S.W. Kurny, F. Gulshan, Parameters affecting the photocatalytic degradation of dyes using TiO₂: A review, *Appl Water Sci*, 7(4), 2017, 1569-1578.
- [12] N.M. Mahmoodi, Z. Mokhtari-Shourijeh, J. Abdi, Preparation of mesoporous polyvinyl alcohol/chitosan/silica composite nanofiber and dye removal from wastewater, *Environ Prog Sustain*, 38, 2018, 100-109.
- [13] G.Z. Kyzas, M. Kostoglu, Green adsorbents for wastewaters: A critical review, *Materials*, 7(1), 2014, 333-364.
- [14] J.Z. Mitrovic, M.D. Radovic, T.D. Andelkovic, D.V. Bojic, A.L.J. Bojic, Identification of intermediates and ecotoxicity assessment during the UV/H₂O₂ oxidation of azo dye Reactive Orange 16, *J. Environ Sci Heal, A* 49(5), 2014, 491-502.
- [15] S. Mishra, A. Maiti, Process optimization for effective biodecolourization of reactive orange 16 using chemometric methods, *J Environ Sci Heal, A* 54(3), 2019, 179-192.
- [16] D. Guimarães, V.A. Leão, Batch and fixed-bed assessment of sulphate removal by the weak base ion exchange resin Amberlyst A21, *J Hazard Mater*, 280, 2014, 209-215.
- [17] Z. Hubicki, A. Wolowicz, Adsorption of palladium (II) from chloride solutions on Amberlyst A 29 and Amberlyst A 21 resins, *Hydrometallurgy*, 96(1-2), 2009, 159-165.
- [18] B. Han, W. Carvalho, L. Canilha, S.S. da Silva, J.B.A.E. Silva, J.D. McMillan, S.R. Wickramasinghe, Adsorptive membranes vs. resins for acetic acid removal from biomass hydrolysates, *Desalination*, 193(1-3), 2006, 361-366.
- [19] S.K. Sari, D. Özmen, Design of optimum response surface experiments for the adsorption of acetic, butyric, and oxalic acids on Amberlyst A21, *J Disper Sci Technol*, 39(2), 2018, 305-309.
- [20] J.M. Karekar, S.V. Divekar, Adsorption studies of chromium (VI) on weak base resins Tulsion A-10X (MP) and Amberlyst A-21 (MP) in aqueous and mixed media, *Desalin Water Treat*, 82, 2017, 252-261.
- [21] S. Nagireddi, A.K. Golder, R. Uppaluri, Role of protonation and functional groups in Pd(II) recovery and reuse characteristics of commercial anion exchange resin-synthetic electroless plating solution systems, *J Water Process Eng*, 22, 2018, 227-238.
- [22] P. Sathishkumar, M. Arulkumar, T. Palvannan, Utilization of agro-industrial waste *Jatropha curcas* pods as an activated carbon for the adsorption of reactive dye Remazol Brilliant Blue R (RBBR), *J Clean Prod*, 22(1), 2012, 67-75.
- [23] F. Kallel, F. Chaari, F. Bouaziz, F. Bettaieb, R. Ghorbel, S.E. Chaabouni, Sorption and desorption characteristics for the removal of a toxic dye, methylene blue from aqueous solution by a low-cost agricultural by-product, *J Mol Liq*, 219, 2016, 279-288.
- [24] V. Janaki, K. Vijayaraghavan, A.K. Ramasamy, K.J. Lee, B.T. Oh, S. Kamala-Kannan, Competitive adsorption of Reactive Orange 16 and Reactive Brilliant Blue R on polyaniline/bacterial extracellular polysaccharides composite-A novel eco-friendly polymer, *J Hazard Mater*, 241-242, 2012, 110-117.
- [25] H. Zhu, T. Chen, J. Liu, D. Li, Adsorption of tetracycline antibiotics from an aqueous solution onto graphene oxide/calcium alginate composite fibers, *RSC Adv*, 8(5), 2018, 2616-2621.
- [26] I. Langmuir, Adsorption of gases on plane surfaces of glass mica and platinum, *J Am Chem Soc*, 40(9), 1918, 1361-1403.
- [27] S.R. Mishra, R. Chandra, J. Kaila, S. Darshi, Kinetics and isotherm studies for the adsorption of metal ions onto two soil types, *Environ Technol Inno*, 7, 2017, 87-101.
- [28] H.M.F. Freundlich, Over the adsorption in solution, *Phys Chem*, 57, 1906, 385-470.
- [29] S. Dadfarnia, A.M.H. Shabani, S.E. Moradi, S. Emami, Methyl red removal from water by iron-based metal-organic frameworks loaded onto iron oxide nanoparticle adsorbent, *Appl Surf Sci*, 330, 2015, 85-93.
- [30] Y.S. Ho, G. Mckay, Pseudo-second order model for sorption processes, *Process Biochem*, 34(5), 1999, 451-465